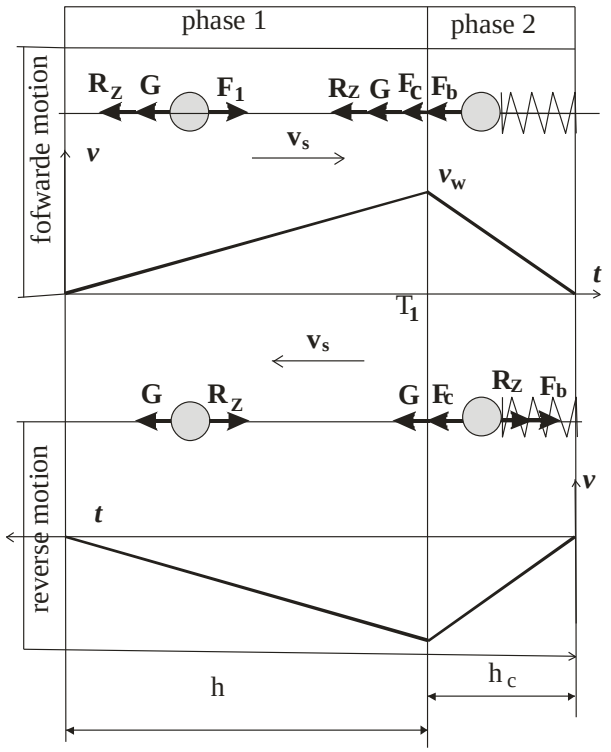

Figure 3. Timing chart of the relocation of the center of mass S relative to the axis $O^0{}_1Z$

Let us consider a forward motion mode. Due to the properties of the aerodynamic profile of the sail, the lifting aerodynamic force F_1 is much higher than the force F_2. This mode is the first to consider because it is crucial for further establishing the working motion of the rod and displacement of the rod under the action of elastic forces. In the analysis of the forward motion mode, in this case the limitation is the motion time which depends on the frequency of the wind pulsation H [9]. Therefore, the forward motion time in the first stage is T_1=H/2 c. The component of the acceleration at the beginning of the first stage is $a_Y = v_W / T_1$. We determine working motion corresponding to the maximum motion:

$h = a_W \cdot T_1^2 / 2$.

Equation (4) is nonlinear, so we will seek an approximate solution in increments of speed and time. For this, we split the action time of wind force into n, equal intervals of time, then produce quantization at the time $\Delta t = T_1 / n$ We assume that an impulse of force depending on the squared speed acts on the center of mass in a finite interval of time. The speed of the sail on each segment of time decreases by the value of the sum of the speed change on the previous segments. This is due to the fact that the expression for the lifting force has a wind speed relative to the sail. At each i-th interval, a lifting force decreasing in magnitude acts on the sail because the relative wind speed decreases. Equation (4) can be represented in the form of a system of equations

$$\Delta v_Z^s = \frac{1}{M}[A_1(v_W - \sum_1^{i-1} \Delta v_{iZ}^s)^2 - G + R_{iZ}]\Delta t \text{ ,i=1,,.n.} \quad (6)$$

Here $A_1 = c_A \cdot \frac{1}{2} \cdot \rho \cdot S_P$, constant;

Expression (6) allows us to determine the vertical component of the speed of the WB's center of mass and of the sail at any time in the first stage of forward motion. Since at the initial moment $v_0^s = 0$, then from (6) we obtain the dependence for the vertical component of the reaction force and its maximum value R_{nZ}.

At the second stage of the forward motion during the movement of the center of mass S, elastic forces $F_c = c\,(z_s\text{-h})$ and damping forces $F_b = b\frac{dz_s}{dt}$ actuators, as well as gravitational forces that impede the motion, act in the direction of the y axis, so the dynamics equation (4) will have the form

$$M\frac{d^2 z_s}{d^2 t} - b\frac{dz_s}{dt} - c(z_s - h) - G + R_{nZ} = 0 \quad (7)$$

where b, c are damping and elastic coefficients; R_{nZ} is the reaction composite force determined from (6) at i=n.

By solving the differential equation (7), given M, b, h, G, R_nZ and initial speed v_W, we determine T_2, motion time at this stage, and c, an elastic coefficient of the damping elements. Assuming that the law of motion is uniformly retarded, we determine h_C movement in the area of stage 2, at which the energy of the elastic elements accumulates.

At the first stage of the reverse motion, the energy of elastic elements is recuperated. The equation of the dynamics of S motion relative to axis O_0Z_0 at this stage is as follows:

$$M\frac{d^2 z_s}{d^2 t} - b\frac{dz_s}{dt} + c(h_c - z_s) + G - R_Z = 0 \quad (8)$$

By solving the differential equation (8), the reaction forces and acceleration at this stage are determined. Given a uniformly accelerated motion, the final speed at the stage v_3 and the reaction force are determined. At the second stage of the reverse motion, motion occurs only under the action of gravity and the reaction force. The speed at this stage changes from the initial value $v_0 = v_3$ to zero, and the distance traveled by the center of mass is known and equal to h.

$$M\frac{d^2 z_s}{d^2 t} + G - R_Z = 0 \quad (9)$$

Solving the inhomogeneous differential equation (7) enables to establish the dependence of the motion of the center of mass in the second stage of the forward motion and the elastic coefficient. In future calculations, the value of the elastic coefficient will be checked. From the

operating conditions of the WPI it follows that in the second stage of the forward motion, the energy of the elastic forces actuators is accumulated which makes it possible to return the working body to the initial position during the reverse motion. In this connection, the elastic coefficient must meet these requirements. In case of noncompliance of the elastic coefficient, the calculation cycle is repeated.

From equation (9) we determine the acceleration. Then, assuming that the motion is uniformly retarded, we determine the v_0 value, the time of the second stage of the reverse motion T_2 and the reaction force R_Z .

From then on, when building a simplified model and making a dynamic analysis of the center of mass relocation with respect to the axis $O^0{}_1Y_0$ (3) and rotation around the axis passing through the point S perpendicular to the plane Q (5), the solutions and arguments given in the analysis of the center of mass motion relative to the axis $O^0{}_1Z_0$ are repeated. As a result, we determine the maximum values of the composite force of reaction R_Y and moment of couple MR. The moment and forces of a reaction acting on the working body from a conditionally "rigidly fixed" platform are the initial ones for force analysis of the MC.

5. Dynamic analysis of the manipulator converter

If we take into account that the sail is influenced by a resultant of aerodynamic forces of wind and gravitational force of the working body, then during cyclic variation of the wind speed and the change of the wind direction, the working body's movement will be spatially closed. With this movement of the upper platform, the lengths of all six telescopic joints will vary. Shown in Figure 4, results of solving a kinematic task for a parallel manipulator in MatLab by the algorithm proposed in [10] demonstrate that during the reverse motion of the movable platform all six rods receive the displacement increment.

To estimate the power of the WPI during the engineering or in operation, data are required on the forces in actuators and the rods motion speed. Force of the cylinder rod along with the motion allow to choose the design of pneumatic and hydraulic cylinders. To determine the forces on the rods, a force analysis of the MC is performed using the kinetostatics method.

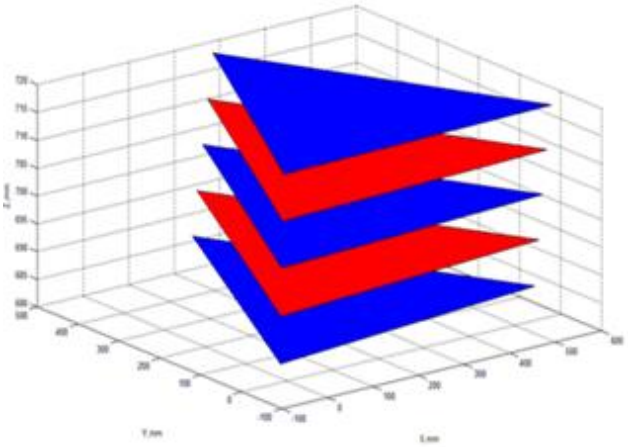

Figure 4. The diagram of location of the working body's upper platform

The initial data is the main vector of the reaction force $\vec{R} = \vec{R}_Z + \vec{R}_Y$ applied at the point O_1 and a vector of a couple of forces $\vec{M}_R$ resulting from the dynamic analysis of the working body under the action of maximum wind speed of 15-20 m/s and with the inertia forces taken into account. It should be noted that the force $\vec{R}$ is located (Figure 5) in the plane Q, and the moment of couple $\vec{M}_R$ is directed perpendicularly to the plane Q which coincides with the moving plane $O_1Y_1Z_1$. Thus, with a given wind direction, the values $\vec{R}$ and $\vec{M}_R$ are known. In addition to these forces, the unknown forces N_3, N_4, N_5, N_6, N_7, N_8 directed along the rods' axes have an effect on platform 2. The directions of the action lines for each position are determined by solving an inverse problem of kinematics.

We choose a fixed coordinate system $O_0\ X_0Y_0Z_0$ connected with the lower platform of the manipulator converter with the beginning in the node C_1. Since $\vec{R}$ and $\vec{M}_R$ comprise the inertia forces the kinetostatics equation for the platform has the following form

$$\sum_{i=3}^{i=8} N_{iz} + R_z = 0; \sum_{i=3}^{i=8} N_{iy} + R_y = 0;$$

$$\sum_{i=3}^{i=8} N_{ix} = 0; \sum_{i=3}^{i=8} M_x(\mathbf{N}_i) + M_{Rx} = 0;$$

$$\sum_{i=3}^{i=8} M_y(\mathbf{N}_i) + M_{Ry} = 0; \sum_{i=3}^{i=8} M_z(\mathbf{N}_i) = 0.$$

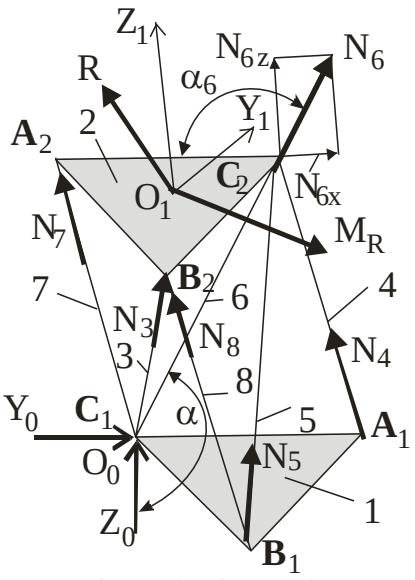

Figure 5. Scheme for the MC force analysis

The obtained values of forces on the MC rod are used later in choosing pneumatic-hydraulic cylinders for the WPI design engineering.

6. A Laboratory-Scale Model of the WPI

To confirm the functional capabilities of the sail WPI and study the sail motion, an acting laboratory-scale model of the WPI has been constructed. The model is shown in Figure 6. Here, the toroidal sail 5 is fixed rigidly to the movable platform 4 of the manipulator converter. Each rod of the "rod-cylinder" connection 2 is connected to the rotor of linear electric generator 3 generating an electric current which is recorded by the micro ammeter unit 6. In the model, the sail was located at a low altitude, in addition, the sail had no aerodynamic profile in cross section and did not change the windage. Nevertheless, this model allowed to demonstrate the principle of functioning of the WPI. Namely, under the influence of the wind force, the sail made spatial movements, depending on the direction and speed of the wind. By doing it, the sail captures the kinetic energy of the air mass, whereas the manipulator converter converts this energy into mechanical energy of the forward motions of six rods relative to the cylinders, which allows to generate electrical energy.

Figure 6. An acting laboratory-scale model of the WPI

It was possible to observe on the model that the sail, moving under the wind force action, simultaneously compresses the spring in the rod-cylinder connection. In the reverse motion, the sail was moved by the spring action. The acting model also showed that the toroidal shape of the sail prevents destructive effect of wind on the working bogy. For example, in high winds the working body was deflected by a maximum angle at which the airflow separation from the sail occurred due to toroidal shape. After the gust of wind stopped, the working body returned to its initial position under the action of elastic forces. At a given wind direction 2-3 telescopic joints were actively functioning. When the wind direction changed, there were other 2-3 telescopic joints. The movement of the working body in the absence of strong gusts of wind was represented by vibrations with a small amplitude. The essential difference between the prototype and the other existing wind power installation is the use of a swinging sail with an automatically controlled windage and a manipulator converter with six degrees of freedom.

7. Conclusion

The article analyzes the aerodynamic variables, timing chart and a built simplified dynamic model of a novel WPI. The study provided a rationale for the methods for determining the geometric dimensions and shape of the sail. The authors determined geometric, kinematic and dynamic properties which are necessary for the future design engineering, as well as for automatic control and research of the wind power installation. It is substantiated that the WPI's working body will perform self-excited vibrations in large. The study gives a description of the acting laboratory-scale model of the WPI.

References

[1] P'yankov K. S., Toporkov M. N. (2014) Mathematical modeling of flows in wind power installation with a vertical axis//Fluid Dynamics, T. 49. № 2. pp. 249-258.

[2] Gasch. R., Twele. J. (2016) Windkraft Langer Grundlagen, Entwurf, Planung und Betrieb/ Springer, XXIII, p. 599.

[3] Apelfröjd S., Eriksson S., Bernhoff H. (2016) A Review of Research on Large Scale Modern Vertical Axis Wind power installation at Uppsala University//Energies, T. 9. № 7. P. 570.

[4] US20140341736A1, (2014) Sail WPI. Nov. 20.

[5] US 2013 0181458A1, (2013) System for converting wind energy. Jul.18.

[6] K.S. Sholanov. Platform robot manipulator. WO/2015/016692,05.02.2015.

[7] K.S. Sholanov. Power plants (variants) on the basis of parallel manipulator. WO/2018/147716, 16.08.2018.

[8] K Tochmetova, K.S. Sholanov. Float converter model for wave power sources. Research Article in EAI Endorsed Transactions on Energy Web **17**(13): e2 http://eudl.eu/issue/ew/4/13 (S 0119).

[9] M.A. Novitskii, L.M. Khachaturova, L.K. Kulizhnikova, M.K. Matskevich, (2007) Maximum fluctuations of wind direction in limited time intervals at the levels up to 300 m from observations at a meteorological tower. Russian Meteorology and Hydrology. T. 32. № 3. pp. 168-175.

[10] K.S. Sholanov, K.A. Abzhaparov, Zh.T. Zhumasheva, M. Ceccarelli, (2016) A new parallel manipulator hydraulically actuated. International Journal of Mechanics and Control, Vol. 17, No. 01, pp. 49-57.